

## Forward lasing action at multiple wavelengths seeded by white light from a femtosecond laser filament in air

Tie-Jun Wang,<sup>1,2,\*</sup> Jean-François Daigle,<sup>3</sup> Jingjing Ju,<sup>1,2</sup> Shuai Yuan,<sup>2</sup> Ruxin Li,<sup>1</sup> and See Leang Chin<sup>2</sup>

<sup>1</sup>State Key Laboratory of High Field Laser Physics, Shanghai Institute of Optics and Fine Mechanics, Chinese Academy of Sciences, China

<sup>2</sup>Département de Physique, de Génie Physique et d'Optique, Centre d'Optique, Photonique et Laser (COPL), Université Laval, Québec, Québec G1V 0A6, Canada

<sup>3</sup>AEREX Avionique Inc., Breakeyville, Québec G0S 1E1, Canada

(Received 23 August 2013; published 27 November 2013)

White-light seeded forward lasing action from a femtosecond laser filament in air was systematically investigated. Using the self-generated white-light seed from 800- and 400-nm laser filaments, 428- and 391-nm lasings, respectively, were observed. When an external white-light seed produced from a femtosecond laser supercontinuum in a water cell was used, simultaneous multiple-wavelength (388-, 391-, 428-, and 471-nm) lasing action was experimentally demonstrated.

DOI: [10.1103/PhysRevA.88.053429](https://doi.org/10.1103/PhysRevA.88.053429)

PACS number(s): 33.80.Rv, 42.65.-k, 52.25.Os, 52.38.Hb

### I. INTRODUCTION

When an intense ultrashort laser pulse propagates in a transparent medium, for instance, in air, an intense light-induced refractive index change will lead to beam self-focusing together with pulse spectral broadening, which is dominated by the optical Kerr response of the medium. Once the pulse peak power is higher than a critical value, namely, the critical power for self-focusing [1], the self-focusing will overcome natural linear diffraction and will collapse, resulting in the tunneling or multiphoton ionization of air molecules. The further evolution of the pulse is governed mainly by a competition between Kerr self-focusing and plasma defocusing together with linear diffraction, group-velocity dispersion, and multiphoton absorption. As a consequence, a plasma channel, referred to as a laser filament, is formed [1–7]. Laser intensity inside air filaments produced from laser pulses at 800 nm is clamped at  $\sim 5 \times 10^{13}$  W/cm<sup>2</sup>, and this intensity drops to  $\sim 2.5 \times 10^{13}$  W/cm<sup>2</sup> when 400-nm laser pulses are used [8]. This femtosecond laser filament with high intensity can be projected for a long distance in the atmosphere. Femtosecond laser filamentation has stimulated many applications, such as new frequency generation from UV to terahertz [9,10], standoff spectroscopy [11], filament-based weather control [12,13], etc. Also, lasing action recently attracted a lot of research interest [14–22].

The high intensity inside a laser filament not only ionizes air molecules, but also excites the molecules and ions into highly lying states leading to characteristic fluorescence. Using a filament as a gain medium, the amplified spontaneous emission (ASE) type of gain from the backward fluorescence of air molecules using 800-nm laser pulses has been reported [14]. This type of lasing was characterized as randomly polarized and incoherent. More recently, by using midinfrared (MIR) laser pulses, generated from an optical parametric amplifier pumped by a Ti:sapphire laser system, coherent and linearly polarized lasing actions from MIR filament-induced ionic N<sub>2</sub> (N<sub>2</sub><sup>+</sup>) [15,16] and ionic CO<sub>2</sub> (CO<sub>2</sub><sup>+</sup>) [17] have been observed. A two-pulse scheme also was reported

to generate this type of lasing, either using a Ti:sapphire laser pulse (centered at  $\sim 800$  nm) together with its second harmonic [18,19] or a femtosecond filamenting pulse with other nanosecond heater pulses [20,21]. All the observations on coherent lasing mentioned above are based on complicated systems (optical parametric amplifier pumped by a Ti:sapphire laser) or complicated experimental schemes (two beams). More recently, we demonstrated the possibility to generate forward lasing from only one air filament of femtosecond Ti:sapphire laser pulses [22]. The mechanism of this forward lasing action is explained as the stimulated amplification of a harmonic seed (third or fifth harmonic) at UV range due to the population inversion generated between two vibrational levels of N<sub>2</sub><sup>+</sup> [23]. However, once the intense filament creates the population inversion between two vibrational levels of N<sub>2</sub><sup>+</sup>, the harmonic seed could be either self-generated from the laser pulse itself or generated from another external source. The only requirement of the seed is to cover the transition wavelength of two vibrational levels of ionic nitrogen in air. With the spectral broadening effect occurring with the filament, namely, white light, can one use it as the seed to create the forward lasing, in particular, to achieve simultaneous multiple wavelength lasing? In this paper, we attempt to answer this question experimentally. We systematically investigate the coherent forward lasing action from a femtosecond laser filament in air. This lasing action can be achieved from a single laser filament either from 800- or from 400-nm-fs laser pulses. Besides that, multiple-wavelength lasing action from an 800-nm laser filament in air has been observed by using laser-induced white light as an external seed.

### II. EXPERIMENTAL SETUPS AND METHODS

The experiments were performed by using a 10-Hz/45-fs/800-nm laser pulse from a commercial Ti:sapphire laser system. Laser-pulse energy can be tuned up to 15 mJ through the combination control of a thin-film polarizer and a half-wave plate inserted before a two-pass amplifier. The beam diameter was  $\sim 1$  cm. Several millijoule-femtosecond blue pulses (400 nm) were generated by frequency doubling the fundamental Ti:sapphire laser pulse using a 100- $\mu$ m-thick  $\beta$ -barium borate crystal. In the experiment using the

\*Corresponding author: [tjwang2007@yahoo.com](mailto:tjwang2007@yahoo.com)

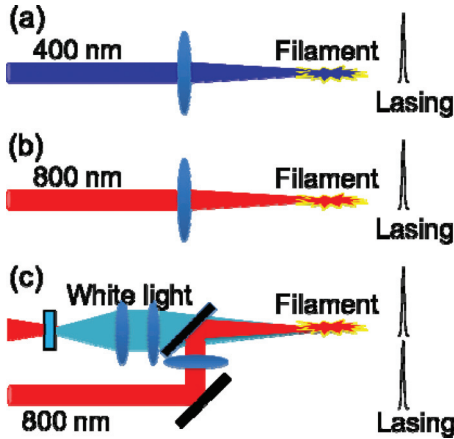


FIG. 1. (Color online) Schematics of experimental setups on forward lasing action from a white-light-seeded laser filament in air. (a) and (b) Lasing action from self-seeded blue (400 nm) and red (800 nm) filaments, respectively, and (c) for externally generated white-light seeding (see text for details).

self-generated white-light seed [Figs. 1(a) and 1(b)], a femtosecond laser filament was created in air after the laser pulse passed through a focusing lens [60 cm in Fig. 1(a) and 22 cm in Fig. 1(b)]. All the transparent optics used in the experiments were UV grade and have good transmission in the UV. In the blue (400-nm) filament case, the forward spectrum at 60 cm after the filament was measured by directly sending the pulse into an integrating sphere that was connected to an intensified CCD (ICCD) spectrometer through a fiber. In the case of the “red” (800-nm) filament, a  $45^\circ$  800-nm mirror was used to filter out the 800-nm filamenting pulses and to let UV emission pass through it. This UV emission then was collected by a 10-cm focal length lens and was sent to the integrating sphere and fiber-coupled ICCD spectrometer. The laser filament-induced fluorescence in both cases [Figs. 1(a) and 1(b)] also was collected, perpendicular to the laser beam propagation axis, by a pair of lenses and was focused to a fiber link connected to the spectrometer. In the experiment of Fig. 1(c), an external white-light seed was generated by focusing part of the 800-nm laser pulses through a 1-cm-long water cell. The water cell was followed by an 800-nm  $45^\circ$  mirror [not shown in Fig. 1(c)] to filter out the strong 800-nm fundamental pulse and to let white light from IR to near-UV pass through it. Another 800-nm  $45^\circ$  mirror was used to couple the filament and white light for collinear propagation. Spatial overlap between the laser filament and the focused white light was controlled by a pair of lenses. A translation stage was built in the white-light path to control the temporal overlap. The UV emission was collected by using the same method that had been used in the experiment of Fig. 1(b). A cubic polarizer was inserted in front of the integrating sphere or fiber head for the emission polarization measurement.

### III. WHITE-LIGHT SELF-SEEDING OF A 400-NM FILAMENT

Since most lasing actions observed from air molecules are from ionic nitrogen ( $N_2^+$ ) in the wavelength range of 300–500 nm, looking for a suitable seed in this spectral range is very crucial. Using an intense 400-nm-fs laser pulse to

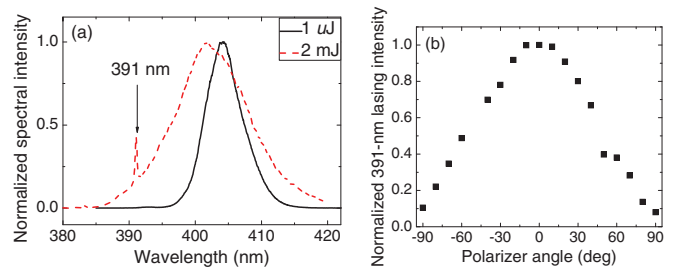


FIG. 2. (Color online) (a) Forward spectra of blue pulses under different energies (1  $\mu$ J in the solid black line and 2 mJ in the dashed red line) and (b) polarization measurement of 391-nm lasing.

create a filament, the generated white-light spectra could reach the UV part ( $<400$  nm) with which self-seeded lasing action could be expected. With this idea in mind, we performed the blue filament experiment. Two-millijoule blue pulses (400 nm) were used to create a filament in air. The forward spectra are shown in Fig. 2(a). The spectrum measured after the focal point is much broader for the 2-mJ pump pulse, which produced a filament, as compared to the 1- $\mu$ J pulse. There is a clear lasing action at 391 nm sitting on the UV extension of the spectrum. Note the forward detection has to be set slightly off axis ( $\sim 1.4^\circ$ ) in order to avoid sending the strong central part of the beam to the integrating sphere. The polarization property is one of the most important parameters to characterize the coherence of optical emission. An emission with a certain polarized direction is strong evidence on lasing action because both spontaneous emission and ASE hold isotropic polarization. The polarization property of the 391-nm lasing has been characterized as shown in Fig. 2(b). An emission linearly polarized in the direction parallel to that of the pump pulse was observed, which is totally different from the randomly polarized fluorescence measured from the side [8]. This also provides strong evidence on the filament-induced white-light seed being amplified. This lasing action is from the transition of two vibrational levels of  $N_2^+$ , which are  $B^2\Sigma_u^+(0)$  to  $X^2\Sigma_g^+(0)$  [24]. The bandwidth of this lasing pulse is  $\sim 0.33$  nm in FWHM, which corresponds to the Fourier-transform-limited pulse duration of 0.68 ps.

### IV. WHITE-LIGHT SELF-SEEDING OF AN 800-NM FILAMENT

As is well known, the white-light spectrum generated from 800-nm air filaments also can cover the UV range of the lasing actions. The significance of only using 800-nm air filaments to achieve the lasing action is very important because one can simplify the generation method by using a powerful Ti:sapphire laser system, which will provide much stronger laser pulses and will cause higher plasma density, leading to potentially higher population inversions of  $N_2^+$ . The possibility of only using single 800-nm air filaments to achieve lasing action has been demonstrated in our previous paper [22]. Here we will provide more details.

The forward spectrum in the blue-UV part after the laser filament is shown in Fig. 3. The pulse energy was fixed at 8 mJ in the measurements. There is only one very strong  $\sim 428$ -nm (427.8-nm) spike sitting on the plateau of the filament-induced white light. This 428-nm emission is from the transition

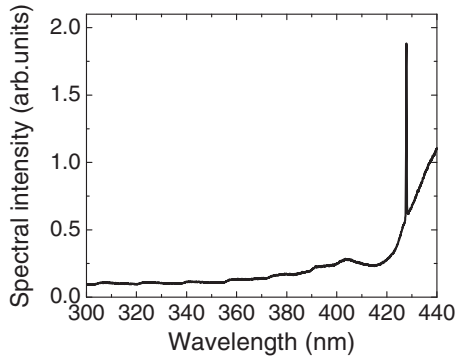


FIG. 3. Typical spectrum from forward detection in the case of only one 800-nm laser filament in air. The pump energy was  $\sim 8$  mJ.

of  $B^2\Sigma_u^+(0)$  to  $X^2\Sigma_g^+(1)$  of  $N_2^+$  [24]. We do not see the typical fluorescence spectrum [11,25,26] covering the signals from the first negative band system of  $N_2^+$  ( $B^2\Sigma_u^+ - X^2\Sigma_g^+$  transition) with the principal wavelengths at 391 and 423 nm and the second positive band system of  $N_2$  ( $C^3\Pi_u - B^3\Pi_g$  transition) with the principal wavelengths at 316, 337, 357, and 380 nm. This is because those fluorescence signals are too weak to detect in the forward direction as compared with the generated strong white light and lasing emission accompanying the filament. The white-light signal at many of the shorter wavelengths must be too weak or nonexistent to be amplified. The behavior of the forward emission in the lasing window of 415–435 nm is shown in Fig. 4(a), obtained using two different pump energies of 2 and 8 mJ. In the case of using the 2-mJ pulses, one can only see the white-light background without any lasing signal. When the pump energy was increased to 8 mJ, not only the white-light signal was enhanced, but also the lasing action was induced. The peak

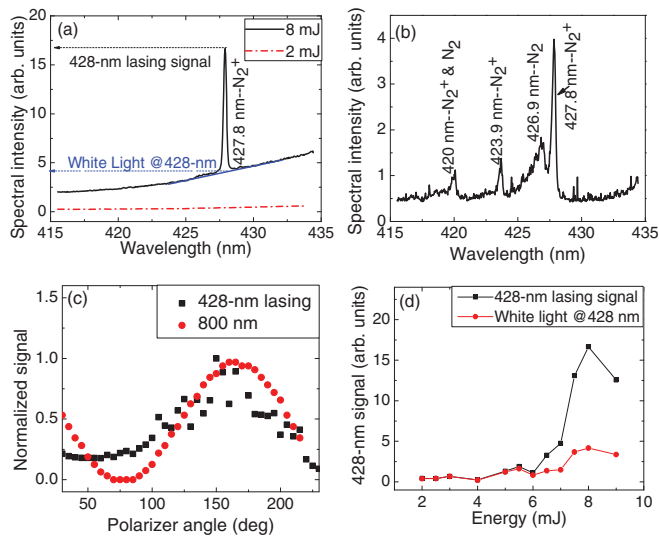


FIG. 4. (Color online) (a) Lasing signals in the spectral range of 415–435 nm under different pump energies (2 mJ in the dashed dotted red line and 8 mJ in the solid black line), (b) fluorescence signal in the same spectral window in (a), (c) the measurements of the polarization property for 428-nm lasing and the 800-nm filamenting pulse, and (d) pump energy dependence of the 428-nm forward lasing action and white light.

signal around 428 nm was chosen as the lasing signal in the following analysis. The intensity of white light at 428 nm also was estimated by using a fit line as shown Fig. 4(a). The spectral spike in Fig. 4(a) is narrow and symmetrical. There are no other lines observed. This is clearly different from the typical fluorescence signal obtained as shown in Fig. 4(b). Both  $N_2$  fluorescence and  $N_2^+$  fluorescence simultaneously are detected over a long time (nanoseconds). In the forward direction [Fig. 4(a)], only the 428-nm transition went through stimulated amplification. The polarization property is a very useful parameter to distinguish the lasing from fluorescence. As shown in Fig. 4(c), the polarization of this 428-nm lasing line has the same polarization property as the pump pulse, which agrees well with the previous observation using the MIR filamenting wavelength [15–17]. Here the polarization of the filamenting pulse (800 nm) was characterized before the laser filaments. This, again, is evidence for 800-nm filament-induced white-light seeding. The bandwidth of this lasing pulse is  $\sim 0.26$  nm at FWHM, which corresponds to the Fourier-transform-limited pulse duration of 1.03 ps. The pump energy dependence of lasing and white light at 428 nm is depicted in Fig. 4(d). Under low filamenting pulse energy ( $< 5$  mJ in our case), there is no lasing action detected. The signal intensities of lasing and white light were considered at the same level. Above a certain value ( $\sim 5$  mJ in our case), the 428-nm lasing signal appeared and grew nonlinearly with increasing 800-nm pulse energy. The higher the filamenting pulse energy was, the stronger the white-light signal at 428 nm was found; the 428-nm lasing line became much stronger. The 428-nm lasing pulse energy was around the submicrojoule level under an  $\sim 8$ -mJ pump through the estimation of the spectral intensity.

## V. LASING FROM AN EXTERNAL WHITE-LIGHT-SEEDED 800-NM AIR FILAMENT

So far, single lasing actions at 391 and 428 nm have been demonstrated by only using 400- and 800-nm air filaments, respectively. The self-generated white-light seed was too weak to be controlled independently. In order to generate a strong well-controlled white light for seeding the lasing action, we focused part of 800-nm pulse energy through a 1-cm-long water cell. After filtering out the strong 800-nm pulse, the forward white-light spectrum detected is shown in Fig. 5(a). This white-light seed is much stronger than the one from the air filament in Fig. 3. Under the same filamenting pulse energy ( $\sim 8$  mJ), multiple-wavelength emissions, namely, 388,

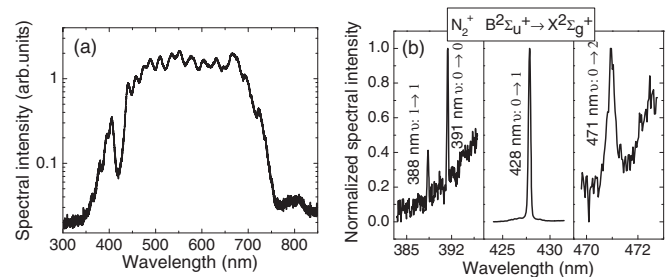


FIG. 5. (a) White-light seed spectrum and (b) simultaneously generated four lasing wavelengths from an external white-light-seeded laser filament in air.

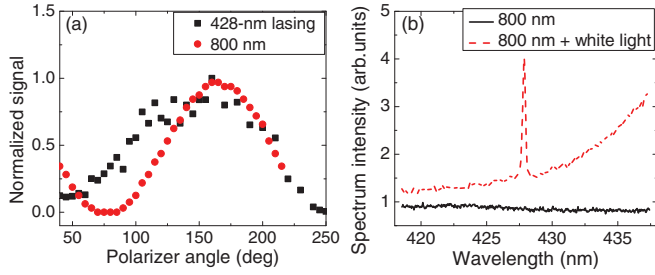


FIG. 6. (Color online) (a) Polarization measurement of 42-nm lasing from an external white-light-seeded 800-nm laser filament in air together with the polarizations of an 800-nm pump and (b) forward spectra around the 428-nm lasing action from the 5-mJ 800-nm laser filament with (dashed red line) and without (solid black line) external white light.

391, 428, and 471 nm, experimentally were demonstrated in this case which are depicted in Fig. 5(b). Polarization of the 428-nm emission shown in Fig. 6(a) was linear and followed the polarization direction of the 800-nm pump pulses, which once again, confirms the coherent lasing actions. The 428-nm lasing also is 1 order of magnitude stronger than that from the self-seeded air filament. The lasing pulse energy could be at microjoule level under an  $\sim 8$ -mJ pump with external white-light seeding through the estimation of the spectral intensity. Among these four detected lasing wavelengths, 428 nm was the strongest, 2 to 3 orders of magnitude stronger than the others. The reason why there was only 428-nm lasing observed in the white-light self-seeded 800-nm air filament is mostly due to the weak self-generated white-light seed. These lasing wavelengths are from the first negative system  $B^2\Sigma_u^+$  to  $X^2\Sigma_g^+$  of  $N_2^+$  [24],

$$B^2\Sigma_u^+(1) \text{ to } X^2\Sigma_g^+(1) \rightarrow 388 \text{ nm,}$$

$$B^2\Sigma_u^+(0) \text{ to } X^2\Sigma_g^+(0) \rightarrow 391 \text{ nm,}$$

$$B^2\Sigma_u^+(0) \text{ to } X^2\Sigma_g^+(1) \rightarrow 428 \text{ nm,}$$

$$B^2\Sigma_u^+(0) \text{ to } X^2\Sigma_g^+(2) \rightarrow 471 \text{ nm.}$$

The bandwidths (FWHM) of those lasing pulses are 0.26 (388), 0.24 (391), 0.28 (428), and 0.26 nm (471 nm), which correspond to the Fourier-transform-limited pulse durations of 0.85, 0.93, 0.96, and 1.25 ps, respectively. In order to confirm the external seeding effect, the forward spectra around the 428-nm lasing action with and without external white light have been recorded as shown in Fig. 6(b). With external white light seeded into 5-mJ 800-nm air filaments, a clear lasing action has been observed. This is strong evidence on white-light-seeded stimulated emission. This principal demonstration of using an externally controllable white-light seed in filament-based laser actions provides more feasibilities to investigate this new frontier.

## VI. PHYSICAL MECHANISM

The forward lasing actions of 388, 391, 428, and 471 nm observed above in three different experiments are identified as the transitions between two vibrational levels of  $N_2^+$ . The mechanism of this white-light-seeded forward lasing action can be ascribed to the stimulated amplification process.

In the case of the self-generated white-light seed, the laser filament (at 800 and 400 nm) plays two roles. On one hand, population inversion between two vibrational levels of ionic nitrogen ( $B^2\Sigma_u^+ - X^2\Sigma_g^+$ ) is created inside the femtosecond laser filament due to the high clamping intensity [23]. On the other hand, filament-induced white light at 391- or 428-nm seeds into these transitions, which stimulated the laser emission at 391 or 428 nm in the forward direction. The white light with its spectral broadening to the blue and UV parts has clearly been confirmed in Figs. 2(a) and 3. Because of the seeding effect, the polarization property of the forward lasing should be the same as that of the white-light seed from 800-nm (400-nm) pump pulses. This is also confirmed by the polarization measurement [Fig. 4(d)]. Since this lasing effect is very sensitive to the intensity of self-generated white-light seeds, which is pump energy dependent, the forward lasing should also depend on the pump energy. At low pump energies, filament-induced white light is rather weak so that this white light cannot cover the seeding wavelength at 300–500 nm. At the same time, the population-inversion effect also is limited, even though population inversion is created once a filament is formed. This forward lasing would be hard to detect. As the pump energy is increased, one can get a longer filament (or even multiple filaments), which will result in the increase in the number of population-inverted ionic molecules. This will lead to the forward lasing occurring much more easily. This forward lasing action is also a highly nonlinear process. Once the filamenting energy is high enough, the lasing signal will be much stronger. This also agrees with our observation. Once a strong white light covering many transitions of  $N_2^+$  vibrational levels was seeded into the air filament, multiple-wavelength lasing action should be expected and successfully demonstrated experimentally.

## VII. CONCLUSION

To summarize, white-light-seeded forward lasing action from a laser filament in air was systematically investigated. This white-light seed, which can cover the transition wavelengths of the vibrational levels of  $N_2^+$ , could be self-generated from the air filament or could be externally generated from the femtosecond laser-induced supercontinuum in a dense transparent material. A 391-nm lasing was observed from self-generated white-light-seeded blue filaments in air. In the experiment of the 800-nm self-seeded air filament, 428-nm lasing was measured. Thanks to the strong well-controlled external white-light seed from water, simultaneous multiple-wavelength (388-, 391-, 428-, and 471-nm) strong lasing successfully was demonstrated from air filaments created by Ti: sapphire laser pulses. Since laser filaments in air induced by 800-nm-fs pulses have been well investigated, in particular, for remote generation and control [7], we believe the lasing techniques reported in this paper will find more applications for remote experiments.

## ACKNOWLEDGMENTS

This work was supported, in part, by NSERC, DRDC—Valcartier, Canada Research Chair, the Canada Foundation for Innovation, the Canadian Institute for Photonics Innovation,

and le Fonds Québécois pour la Recherche sur la Nature et les Technologies. T.-J.W. also acknowledges the support from

the 100 Talent Program of the Chinese Academy Sciences. We thank M. Martin for technical support.

- 
- [1] S. L. Chin, *Femtosecond Laser Filamentation* (Springer, New York, 2010).
- [2] S. L. Chin, S. A. Hosseini, W. Liu, Q. Luo, F. Théberge, N. Aközbeke, A. Becker, V. P. Kandidov, O. G. Kosareva, and H. Schroeder, *Can. J. Phys.* **83**, 863 (2005).
- [3] A. Couairon and A. Mysyrowicz, *Phys. Rep.* **441**, 47 (2007).
- [4] L. Bergé, S. Skupin, R. Nuter, J. Kasparian, and J.-P. Wolf, *Rep. Prog. Phys.* **70**, 1633 (2007).
- [5] J. Kasparian and J.-P. Wolf, *Opt. Express* **16**, 466 (2008).
- [6] V. P. Kandidov, S. A. Shlenov, and O. G. Kosareva, *Quantum Electron.* **39**, 205 (2009).
- [7] S. L. Chin, T.-J. Wang, C. Marceau, J. Wu, J. S. Liu, O. Kosareva, N. Panov, Y. P. Chen, J.-F. Daigle, S. Yuan, A. Azarm, W. W. Liu, T. Saideman, H. P. Zeng, M. Richardson, R. Li, and Z. Z. Xu, *Laser Phys.* **22**, 1 (2012).
- [8] J.-F. Daigle, A. Jaroń-Becker, S. Hosseini, T.-J. Wang, Y. Kamali, G. Roy, A. Becker, and S. L. Chin, *Phys. Rev. A* **82**, 023405 (2010).
- [9] F. Théberge, M. Châteauneuf, V. Ross, P. Mathieu, and J. Dubois, *Opt. Lett.* **33**, 2515 (2008).
- [10] T.-J. Wang, S. Yuan, Y. Chen, J.-F. Daigle, C. Marceau, F. Théberge, M. Châteauneuf, J. Dubois, and S. L. Chin, *Appl. Phys. Lett.* **97**, 111108 (2010).
- [11] S. L. Chin *et al.*, *Appl. Phys. B* **95**, 1 (2009).
- [12] P. Rohwetter, J. Kasparian, K. Stelmasczyk, Z. Hao, S. Henin, N. Lascoux, W. M. Nakaema, Y. Petit, M. Queisser, R. Salamé, E. Salmon, L. Wöste, and J.-P. Wolf, *Nat. Photonics* **4**, 451 (2010).
- [13] J. Ju, J. Liu, C. Wang, H. Sun, W. Wang, X. Ge, C. Li, S. L. Chin, R. Li, and Z. Xu, *Opt. Lett.* **37**, 1214 (2012).
- [14] Q. Luo, W. Liu, and S. L. Chin, *Appl. Phys. B* **76**, 337 (2003).
- [15] J. P. Yao, B. Zeng, H. L. Xu, G. H. Li, W. Chu, J. L. Ni, H. S. Zhang, S. L. Chin, Y. Cheng, and Z. Z. Xu, *Phys. Rev. A* **84**, 051802(R) (2011).
- [16] J. L. Ni, W. Chu, H. S. Zhang, C. R. Jing, J. P. Yao, H. L. Xu, B. Zeng, G. H. Li, C. J. Zhang, S. L. Chin, Y. Cheng, and Z. Z. Xu, *Opt. Express* **20**, 20970 (2012).
- [17] W. Chu, B. Zeng, J. P. Yao, H. L. Xu, J. L. Ni, G. H. Li, H. S. Zhang, F. He, C. R. Jing, Y. Cheng, and Z. Z. Xu, *Europhys. Lett.* **97**, 64004 (2012).
- [18] J. P. Yao, G. H. Li, C. R. Jing, B. Zeng, W. Chu, J. L. Ni, H. S. Zhang, H. Q. Xie, C. J. Zhang, H. L. Li, H. L. Xu, S. L. Chin, Y. Cheng, and Z. Z. Xu, *New J. Phys.* **15**, 023046 (2013).
- [19] J. L. Ni, W. Chu, C. R. Jing, H. S. Zhang, B. Zeng, J. P. Yao, G. H. Li, H. Q. Xie, C. J. Zhang, H. L. Xu, S. L. Chin, Y. Cheng, and Z. Z. Xu, *Opt. Express* **21**, 8746 (2013).
- [20] P. R. Hemmer, R. B. Miles, P. Polynkin, T. Siebert, A. V. Sokolov, P. Sprangle, and M. O. Scully, *Proc. Natl. Acad. Sci. USA* **108**, 3130 (2011).
- [21] P. Sprangle, J. Penano, B. Hafizi, D. Gordon, and M. Scully, *Appl. Phys. Lett.* **98**, 211102 (2011).
- [22] T.-J. Wang, J. Ju, J.-F. Daigle, S. Yuan, R. Li, and S. L. Chin, *Laser Phys. Lett.* **10**, 125401 (2013).
- [23] S. L. Chin, H. L. Xu, Y. Cheng, Z. Z. Xu, and K. Yamanouchi, *Chin. Opt. Lett.* **11**, 013201 (2013).
- [24] R. W. B. Pearse and A. G. Gaydon, *The Identification of Molecular Spectra*, 4th ed. (Chapman and Hall, New York, 1976).
- [25] A. Talebpour, S. Petit, and S. L. Chin, *Opt. Commun.* **171**, 285 (1999).
- [26] A. Talebpour, M. Abdel-Fattah, A. D. Bandrauk, and S. L. Chin, *Laser Phys.* **11**, 68 (2001).